

# An Optimized Thermo-Reflectance Technique for Thermal Conductivity Measurements of Thin-Film Electronic Materials

Mihai G. BURZO, Pavel L. KOMAROV, and Peter E. RAAD

## ABSTRACT

This article presents an overall evaluation of the transient thermo-reflectance technique as applied to the measurement of thermal properties of electronic materials. First, a specific highly-effective implementation of the method is presented. Then, the focus is placed on a systematic characterization of the performance of the thermorefectance technique in which the influences of the most important system parameters on the accuracy of the TTR measurements are ascertained [1]. Finally, the power of the TTR measurement technique and its optimization are demonstrated through representative measurements, first of bulk materials [2] and then of thin-film materials. The experimental investigations address the effects of doping, isotopic purity, interface resistance, deposition/growing methods, and film thickness on the thermal properties of the selected bulk and thin-film layers.

## INTRODUCTION

The continual high demands in modern consumer and industrial electronics have pushed the manufacturing of ICs to unforeseen scientific and technological limits. Miniaturization leads to increased heat generation densities, requiring sophisticated thermal analyses. In order for numerical analysis to be useful in the prediction of performance and reliability of integrated circuits, accurate thermal property data are required. With the drop of the thickness of thin-films into the submicron regime came the realization that bulk and thin-film thermal properties differ noticeably [3]. However, since no universal behavior is expected for these differences and since they cannot be predicted from theory [4], the properties of each material must be measured separately. Since deposition techniques differ by manufacturer, it is important to measure the properties of deposited film *in situ* [5]. Also, as films are typically layered, and the tendency is to use thinner films of higher thermal conductivities, a point is reached where the intrinsic thermal resistance of each film is comparable to the interface resistance between the stacked layers, thus making essential the measurement of such interface thermal resistances.

Among measurement approaches, optical non-contact techniques, such as the transient thermo-reflectance method (TTR) [6], are desirable. The main advantage of the TTR method is that it is a non-contacting and non-destructive optical approach, both for heating a sample under test and for probing the variations of its surface temperature [7]. Until recently, the main drawback of the TTR method has

---

<sup>†</sup> Department of Mechanical Engineering, Southern Methodist University, Dallas, TX 75275-0337, U.S.A., praad@smu.edu, Tel +1-214-768-3866, Fax +1-214-768-4998

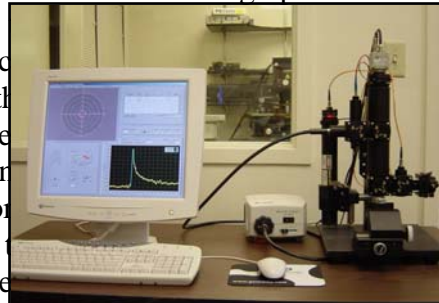
been its extreme sensitivity to hardware and design of samples under test. For example, when measuring transparent materials investigators ended up depositing an opaque absorption layer on top to absorb the heating laser radiation. Taking a broader view, one can say that TTR measurements can be hindered by less-than-desirable optical properties of the top layer material (i.e., low thermo-reflectance coefficient, low reflectivity, high transparency, surface roughness), which degrade the measurement performance of a given system. To eliminate these difficulties, investigators have resorted to the use of the absorption layer on top of the material under test. Metal films are used because they exhibit high absorptivity and their optical properties are usually well known (e.g., Au in [8], Al in [9, 10] and Mo in [10]). The optimum thickness of the absorption layer can be determined by the use of an optimization approach, as will be described later in this article.

## TTR MEASUREMENT TECHNIQUE AND SYSTEM

The basic principle of the transient thermal reflectance method is to heat a sample by laser irradiation and probe the changes in the surface reflectivity of the heated material. The source of energy in the TTR method is normally provided by a pulsed laser with short pulse duration. During each pulse, a given volume below the sample surface heats up due to the absorbed laser light energy. The depth of the volumetric heating is determined by the optical penetration depth, which is a function of laser wavelength and surface material properties. After each laser pulse, the sample cools down to the initial ambient temperature. During this process, a probing CW laser light reflected from the sample surface at the heating spot center is collected on a photodetector (1 ns maximum rise time) to measure the surface reflectivity. The changes in surface reflectivity are proportional to the changes in surface temperature with a time constant in the range [11], are recorded by an oscilloscope (at rate

The result of the experiment is a transient response which represents the overall heat transfer behavior of the unknown material under test. To extract the unknown material properties from the recorded temperature response, an identical mathematical problem is solved numerically with guessed thermal properties with the intention of matching the experimental and numerical transient normalized temperature responses. A mathematical optimization technique makes it possible to systematically vary the desired unknown properties and compare each resulting numerically-obtained response to the reference experimental data until the error between them is minimized in the RMS sense. The final numerical solution hence yields the desired unknown parameters, which represent the best fit to the actual thermal properties of the physical sample. By using a two-parameter optimization technique, the method described in this work yields not only the thermal conductivity of the material under test but also the interface resistance between this material and the absorption layer on top of it.

Figure 1 shows a schematic and picture of the second generation experimental system used to obtain the transient thermo-reflectance (TTR) measurements herein. The heating source is an Nd:YAG pulsed laser with 30 Hz repetition rate, 532 nm



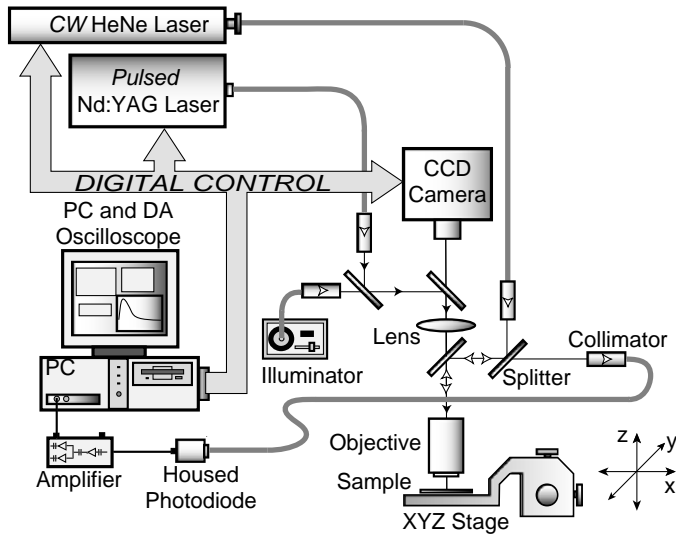


Figure 1. Schematic and picture of the TTR experimental system built at SMU

wavelength, 6.1 ns pulse duration and up to 0.5 mJ pulse energy. A HeNe CW laser with 632 nm wavelength is used for probing. The heating and probing spot dimensions for a 20X objective lens are around 200  $\mu\text{m}$  and 15  $\mu\text{m}$ , respectively.

## METHOD OPTIMIZATION

Maximizing the performance of TTR measurements can be approached from two equally important perspectives. First, the TTR setup itself can be optimized, by adjusting the various characteristics of the components of the TTR system. The most important parameters are the pulse-width of the heating light source and the wavelengths of both the heating and probing light sources. Second, the TTR measurements can be optimized through proper adjustments of the structure and geometry of the sample under test. It is desirable to use a metallic coating on tested samples, but an optimal thickness of coating should be used in order to attain the best performance of the TTR setup. If the absorption layer thickness is not properly chosen, the performance of the TTR measurements of a coated sample could be lower than those of an uncoated sample.

Since the TTR system consists of the heating subsystem delivering power to initiate a temperature response, and the probing subsystem tracking a change in reflectivity of the sample corresponding to the temperature response, the authors have introduced an overall performance coefficient,  $\eta = R_{s_K} \times C_{TR}$ , which can be used to characterize the quality of a thermal conductivity measurement system. The first parameter in the product,  $R_{s_K}$ , represents the responsivity of the TTR thermal conductivity measurements, which characterizes the sensitivity of the temperature response to heat generation and transfer within a sample. The second parameter,  $C_{TR}$ , is the thermorefectance coefficient of the sample surface, which characterizes the signal-to-noise ratio in the reflectivity measurements.

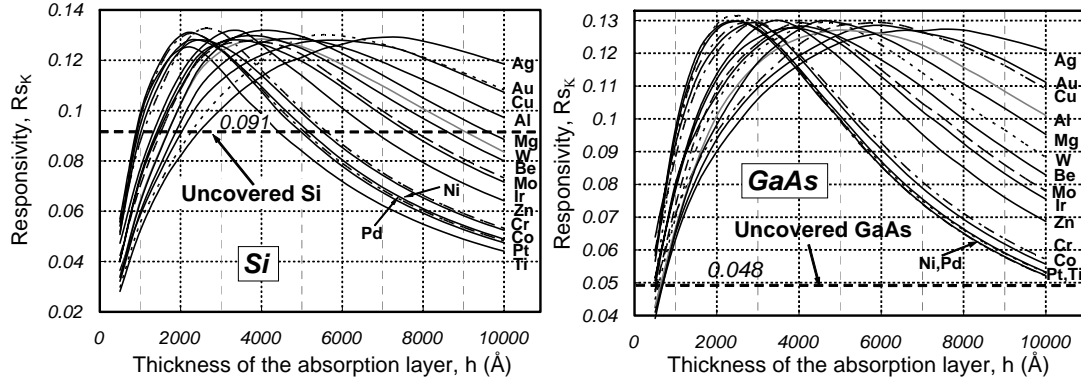


Figure 2. Responsivity of bulk: (a) Silicon and (b) Gallium Arsenide

### Responsivity of the TTR Measurements

The responsivity,  $Rs_K$ , of the thermal conductivity measurement is defined as  $Rs_K = K(d\Theta/dK)_{max}$ , where  $\Theta$  is the normalized temperature response of the sample surface and  $K$  is the thermal conductivity of the material. The responsivity  $Rs_K$  is calculated at the non-dimensional time  $T$  where  $d\Theta/dK$  is maximized. Indeed,  $Rs_K$  is directly connected with the accuracy of the method by the equation  $\sigma_K = Rs_K^{-1} \sigma_\Theta$ , where  $\sigma_K$  is the random measurement uncertainty of the thermal conductivity,  $K$ , and  $\sigma_\Theta$  is the random apparatus uncertainty related to detecting the temperature response. While  $\sigma_\Theta$  depends on the apparatus signal-to-noise ratio and can be considered as a conservative value for a particular setup, the latter equation shows that the measurement uncertainty,  $\sigma_K$ , of the TTR technique decreases with increases in the responsivity value,  $Rs_K$ . Hence, the responsivity,  $Rs_K$ , which depends on the properties and geometry of the materials making up a sample, and the TTR system parameters, can characterize the performance of the TTR method and be useful for optimizing a given experiment. By solving the heat equation for  $\theta$ , it is possible to compute  $Rs_K$  and to bring out important aspects used to assess the performance of the TTR technique (see [17] for a detailed uncertainty analysis).

The calculated responsivities of a bulk silicon sample and a bulk gallium arsenide sample covered with various layers of metals are shown in Figures 2(a) and 2(b), respectively. Only metal films were investigated because they exhibit high absorptivity and their optical properties are usually well known. The responsivity of the uncovered samples is also shown in Figure 2 as a horizontal dashed line ( $Rs_K = 0.091$  for Si and  $Rs_K = 0.048$  for GaAs). The responsivity of measuring metal-covered silicon samples is higher than the responsivity of the uncovered sample if the thickness of the metallic coating is between 2,500Å and 5,000Å. Covering the GaAs sample with any of the 16 metals considered here will produce a significant improvement in the responsivity. The thickness of the absorption layer needs to be precisely controlled in order to achieve the maximum accuracy of the TTR measurements. For example, depositing 6000Å of gold or copper on GaAs will more than double the responsivity of the TTR thermal conductivity measurements.

## The Thermo-Reflectance Coefficient

The sensitivity of the thermorefectance technique is determined by the extent of the change in the reflectivity with changes in the temperature. The measure of this variation is called the thermorefectance coefficient,  $C_{TR}$ . For materials used in electronic devices, the values of the thermorefectance coefficient vary over several orders of magnitude above and below  $10^{-4} \text{ K}^{-1}$ . Furthermore, the thermorefectance coefficient varies widely with the wavelength of the light irradiation used for probing the change in the reflectivity of the sample.

Since the signal-to-noise ratio is directly proportional to the thermorefectance coefficient, when looking into increasing the performance of the TTR measurements, one should choose the probing light source that will yield the maximum thermorefectance coefficient. However, numerical values of  $C_{TR}$  for specific materials over a wide range of laser wavelengths are scarce or nonexistent in the literature. So, one must measure  $C_{TR}$  *in situ* for a specific material at different wavelengths. The authors have developed a system specifically designed for this task, and will report on their measurements in future publications.

As depicted in Figure 3, the change in the thermorefectance coefficient with wavelength does not exhibit a systematic behavior [12-14]. First, the  $C_{TR}$  coefficient is highly dependent on the wavelength of the probing irradiation, as expected. Perhaps less anticipated, however, is the fact that the magnitude of the variations is significant even for small changes in wavelength. Second, practically for all metals,  $C_{TR}$  exhibits a change in sign for certain values of the wavelength.

## The overall Performance Coefficient of the TTR Measurements

The following overall performance coefficient is proposed to characterize the performance of the TTR measurements:  $\eta = R s_K \times |C_{TR}|$ . To minimize the uncertainty of the TTR measurements the above-defined coefficient must be maximized. The coefficient  $\eta$  has been computed using the specific characteristics of the TTR system built at SMU, namely for a HeNe probing laser (632 nm) and a YAG heating laser with a pulse-width of 6.1 ns and wavelength of 532 nm, and is plotted in Figure 4 for a bulk silicon sample covered with a copper, aluminum, or silver absorption layer. It is evident that a layer of copper (5,500Å) will produce the minimal

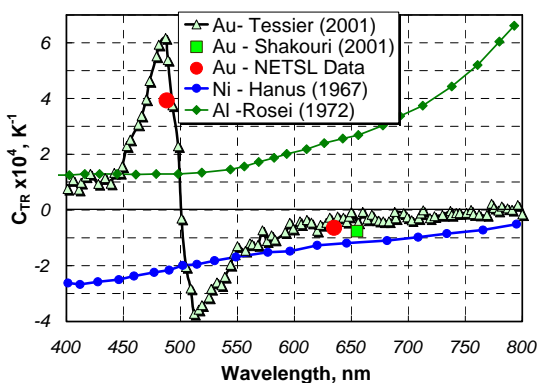


Figure 3. Thermorefectance coefficient [12-14]

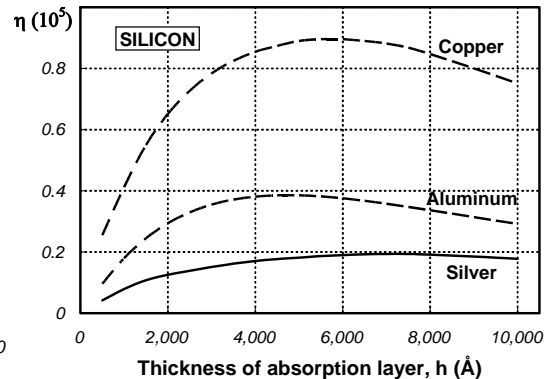


Figure 4. Overall performance coefficient

uncertainty of the TTR measurements.

Surprisingly, the results shown here indicate that in order to achieve the best responsivity of thermal conductivity measurement using a TTR system, any metal can be used to cover a semiconductor or amorphous dielectric sample, as long as the optimum thickness is deposited. Therefore, in order to obtain the smallest uncertainty one should use an absorption layer that maximizes  $C_{TR}$  and then compute the optimum thickness of that layer by maximizing the responsivity of the TTR system.

The results presented herein are useful in two important ways. First, when one is designing a new TTR system, this work can be used to choose the best possible probing and heating lasers. This is especially helpful when measuring samples of similar nature (e.g., measuring the thermal conductivity of materials embedded in a device using gold contacts as an absorption layer). Second, for existing TTR systems, one can use the results of this work to fully design the TTR measurements (i.e., test samples). Specifically, the present study will help one decide on the metal that needs to be used as an absorption layer. The appropriate thickness of the absorption layer can be then calculated using the results presented here. Certainly, there is also a third inherently instructive value to gaining a fuller understanding of the overall efficiency of the thermo-reflectance measurement technique.

## MEASUREMENT RESULTS

### Bulk Materials

The TTR method was used to measure (i) the thermal conductivity of natural silicon and isotopically-pure silicon-28 layers that are epitaxially grown on natural silicon substrates; (ii) the thermal conductivity of the oxide of natural and isotopically-pure silicon; and (iii) the influence of doping type and level on the thermal conductivity at room temperature (300 K).

Seven 4-inch, 635  $\mu\text{m}$ -thick, silicon wafers with a 5  $\mu\text{m}$ -thick epitaxial layer of either natural silicon or isotopically-pure silicon-28 (TABLE I) were considered in this investigation. All samples were covered by a gold layer. The measured values of the thermal conductivity for the epitaxial material and the thermal interface resistance between the gold and epitaxial layers for the seven samples are presented in

TABLE I. THERMAL CONDUCTIVITY AND INTERFACE RESISTANCE MEASUREMENTS

Sample	Material	Doping Type	Doping Level	Gold Cover ( $\text{\AA}$ )	$K \pm \sigma$ (W/m-K)	$R_{th} \times 10^9 \pm \sigma$ ( $\text{m}^2\text{-K/W}$ )
1	Si	Boron (P)	Low ( $1 \cdot 10^{16}$ )	$4,070 \pm 25$	$148 \pm 8.6$	$7.4 \pm 0.23$
2	Si	Boron (P)	High ( $2 \cdot 10^{19}$ )	$4,010 \pm 25$	$122 \pm 7.4$	$6.5 \pm 0.92$
3	$\text{Si}^{28}$	Boron (P)	Low ( $1 \cdot 10^{16}$ )	$5,130 \pm 25$	$227 \pm 12.9$	$5.5 \pm 0.37$
4	$\text{Si}^{28}$	Boron (P)	High ( $2 \cdot 10^{19}$ )	$5,010 \pm 25$	$190 \pm 5$	$5.5 \pm 0.57$
5	Si	Phosphorus (N)	High ( $2 \cdot 10^{19}$ )	$5,040 \pm 25$	$125 \pm 4.8$	$5.8 \pm 0.46$
6	$\text{Si}^{28}$	Phosphorus (N)	High ( $2 \cdot 10^{19}$ )	$5,120 \pm 25$	$194 \pm 12.6$	$5.6 \pm 0.24$
7	Si	Phosphorus (N)	Low ( $3 \cdot 10^{13}$ )	$4,960 \pm 25$	$150 \pm 4.6$	$10.6 \pm 0.36$

the two rightmost columns of TABLE I, along with the associated percentage uncertainty values. The uncertainty values for each measured silicon and Si<sup>28</sup> sample were obtained by calculating the standard deviation of at least 5,000 measured temperature responses. The uncertainty values for the oxide covered sample were obtained by calculating the standard deviation of twenty measurement trials, each consisting of 2,000 measured temperature responses at the same physical location. The average uncertainty in the thermal conductivity is around 5%, while for the interface resistance, the average uncertainty is around 7%.

The effects of isotopic purity, dopant level, and dopant type on the thermal conductivity are presented in terms of percentage changes in TABLE II. Isotopically-pure silicon (Si<sup>28</sup>) is appreciably (55%) more thermally conductive than the natural silicon, both at the lower as well as at the higher levels of doping, for both n-type and p-type doping [2]. The effect of doping level on the thermal conductivity of Si<sup>28</sup> is similar to that observed with both the p-doped and n-doped natural Si samples and is a decrease of ~18% in the thermal conductivity. The effect of doping *type* on the thermal conductivity of the samples investigated here is undetectable within the uncertainty of the TTR measurements. Thus, the qualitative and quantitative behaviors of the n-type and p-type dopants on the thermal conductivity are identical.

## Thin-Films

Thermal properties of thin films, such as SiO<sub>2</sub>, can vary considerably from bulk values. Thus, a better understanding by direct measurement of those properties (as well as the interface resistance between SiO<sub>2</sub> and adjacent layers) is critical. In this section, TTR thermal measurements are shown for thin-film SiO<sub>2</sub> layers.

TABLE II. EFFECTS OF ISOTOPIC PURITY, DOPING LEVEL, AND DOPING TYPE ON THERMAL CONDUCTIVITY

Compared Samples	Reference Sample	Compared Sample	Mathematical Expression	Change in K (%)
1 & 3	Low p-doped <i>Natural Si</i>	Low p-doped Si <sup>28</sup>	$(K_3 - K_1)/K_1$	54%
2 & 4	High p-doped <i>Natural Si</i>	High p-doped Si <sup>28</sup>	$(K_4 - K_2)/K_2$	56%
5 & 6	High n-doped <i>Natural Si</i>	High n-doped Si <sup>28</sup>	$(K_6 - K_5)/K_5$	55%
1 & 2	<i>Low</i> p-doped Natural Si	<i>High</i> p-doped Natural Si	$(K_2 - K_1)/K_1$	-18%
3 & 4	<i>Low</i> p-doped Si <sup>28</sup>	<i>High</i> p-doped Si <sup>28</sup>	$(K_4 - K_3)/K_3$	-20%
7 & 5	<i>Low</i> n-doped Natural Si	<i>High</i> n-doped Natural Si	$(K_5 - K_7)/K_7$	-17%
1 & 7	Low <i>p-doped</i> Natural Si	Low <i>n-doped</i> Natural Si	$(K_7 - K_1)/K_1$	1.4%
2 & 5	High <i>p-doped</i> Natural Si	High <i>n-doped</i> Natural Si	$(K_5 - K_2)/K_2$	2.5%
4 & 6	High <i>p-doped</i> Si <sup>28</sup>	High <i>n-doped</i> Si <sup>28</sup>	$(K_6 - K_4)/K_4$	2.1%

A total of 20 silicon samples were divided into four sets of five samples each. Silicon oxide was thermally grown (TG) on two sets and ion-beam sputtered (IBS) on the other two. One set of each type of SiO<sub>2</sub> samples was covered with a thin layer (100 ± 30 Å) of Cr. Finally, all the samples were covered with a layer of Au (with an optimum, pre-computed thickness of Au). The thickness of the gold layer was chosen such that the uncertainty of the TTR system is minimized.

The measurement procedure used to determine the thermal conductivity of the oxide layer ( $K_{film}$ ) and the thermal interface resistance ( $R_I$ ) was as follows. The samples were tested using the TTR setup to find the transient surface temperature. The geometric and optical parameters were tested independently using the profiler and ellipsometer. Next, the acquired TTR temperature response was matched by the solution of the heat equation by varying the thermal resistance caused by the silicon dioxide layers,  $R_{th}$ . The thermal resistance  $R_{th}$  was then plotted versus the thickness of silicon dioxide. The  $R_{th}$  plot was extrapolated to zero thickness of SiO<sub>2</sub> and the intercept, which represents the interface thermal resistance, was estimated. The slope of the  $R_{th}$  versus  $h$  line, which represents the inverse of the intrinsic thermal conductivity of the SiO<sub>2</sub> film, was also extracted.

For TG SiO<sub>2</sub> films, the interface thermal resistance was found to be  $R_I = 1.68 \times 10^{-8} \text{ m}^2\text{-K/W}$ . When a Cr film was deposited between the gold layer and the thermally grown oxide, the interface thermal resistance of the TG SiO<sub>2</sub> films decreased to  $R_I = 0.78 \times 10^{-8} \text{ m}^2\text{-K/W}$ . For IBS silicon oxide films, the interface thermal resistance was found to be  $R_I = 2.58 \times 10^{-8} \text{ m}^2\text{-K/W}$ , and when a thin Cr layer was deposited between the oxide and the metallization layer, the value of the interface thermal resistance was reduced to  $R_I = 1.15 \times 10^{-8} \text{ m}^2\text{-K/W}$ . Given the above, one may conclude that (a) the interfacial resistance was dependent on the film fabrication process, and (b) a thin layer of Cr deposited between the metal and the dielectric layer will result in more than a two-fold decrease in the interface resistance. Similar reductions in the interface resistance by the use of ultra-thin layers (50Å to 150Å) of other metals (e.g., Ni, Ti, Ni-Cr alloys) have not been investigated, but were expected since such thin layers improve the adhesion of the metallization layer to the underlying dielectric.

From the standpoint of thermal management of electronic devices, the effective thermal conductivity  $K_{eff}$  is the most useful parameter since it is required in engineering computations. Thus, it is beneficial to investigate the variation of  $K_{eff}$  of the SiO<sub>2</sub> layer as a function of the thickness of that layer,  $h$ . The effective thermal conductivity  $K_{eff}$  can be computed as  $K_{eff} = [1/K_{int} + R_I/h]^{-1}$ , where  $K_{int}$  is the intrinsic thermal conductivity of the film,  $R_I$  is the interface thermal resistance and  $h$  is the thickness of the silicon dioxide film. A plot shown  $K_{eff}$  is presented in Figure 5 for both TG and IBS silicon oxide layers (with and without an interfacial Cr layer). The solid curves in Figure 5 represent a polynomial fit of the corresponding effective thermal conductivity data. As expected, a significant decrease in the effective conductivity of the film is observed with the decrease in the thickness of the SiO<sub>2</sub> layer.

Once the effective thermal conductivity and the interface resistance are known, the intrinsic thermal conductivity of the deposited films  $K_{int}$ , can be easily computed from the equation (definition of thermal resistance):  $R_{th} = h/K_{eff} = h/K_{int} + R_I$

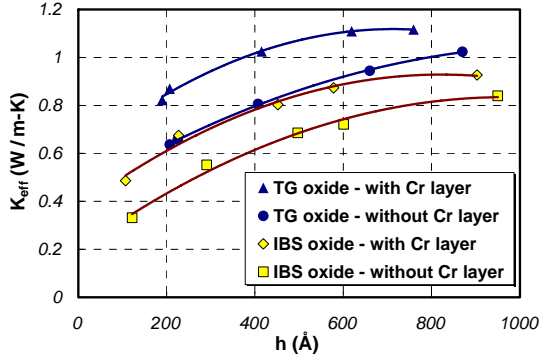


Figure 5. Effective thermal conductivity ( $K_{eff}$ ) vs. thickness of  $\text{SiO}_2$  layer, ( $h$ ).

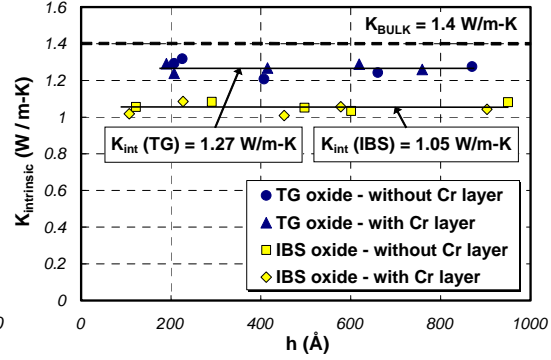


Figure 6. Intrinsic thermal conductivity of  $\text{SiO}_2$  film ( $K_{int}$ ) vs. its thickness ( $h$ ).

where  $h$  is the thickness of the oxide layer,  $K_{eff}$  is the effective thermal conductivity of the oxide layer, and  $K_{int}$  is the intrinsic thermal conductivity of the oxide.

The resulting intrinsic thermal conductivity is shown in Figure 6, and indicates that the intrinsic thermal conductivity of the thin dioxide films tested here is indeed thickness-independent and is less than the value reported in the literature for the bulk silicon oxide  $K_{bulk} = 1.4 \text{ W/m-K}$ . The intrinsic thermal conductivity of the TG oxide tested here is found to be around 90% of the widely published value, while the intrinsic thermal conductivity of the IBS silicon oxide is about 75% of the published value. Specifically, the average intrinsic thermal conductivity of the TG silicon oxide layers is  $K_{int}^{TG} = 1.27 \pm 0.05 \text{ W/m-K}$  and the intrinsic thermal conductivity of the IBS silicon oxide layers is  $K_{int}^{IBS} = 1.05 \pm 0.04 \text{ W/m-K}$ , for thin-film silicon dioxide layers whose thicknesses are between  $100 \text{ \AA}$  and  $1000 \text{ \AA}$ . The values of  $K_{eff}$  and  $K_{int}$  presented above show that thermal transport properties of the  $\text{SiO}_2$  layer are indeed dependent on the method used to deposit the film.

## CONCLUSIONS

In this work several relevant measurement results were presented with the purpose of addressing a number of important issues associated with the thermal properties of electronic materials as well as the TTR methodology itself. A systematic characterization of the performance of the thermoreflectance technique was made by addressing the impact of the parameters of the measurement system as well as the geometry and composition of the sample under test. TTR measurement results were presented with emphasis on the effects of doping, isotopic purity, interface resistance (use of glue-layers), deposition/growing method, and film thickness on the thermal characteristics of bulk and thin-film layers.

An approach for optimizing the TTR measurement of thermal properties was presented. The influence of the most important parameters of the system on the accuracy of the TTR measurements were investigated and discussed. An overall performance criterion was defined based on the responsivity of a given system and the thermoreflectance coefficient of the sample under test. It was shown that in order to obtain the smallest measurement uncertainty one should use a metallic absorption

layer with the highest possible thermorefectance coefficient and then compute the optimum thickness of that layer by maximizing the responsivity of the TTR system.

Measurement results were presented both for bulk and thin-film layers. In order to study the effects of doping and isotopic purity, the TTR method has also been used to measure the thermal conductivity of bulk natural silicon and isotopically-pure silicon-28 layers. Thermal property measurements of silicon dioxide films were also carried out with the optimized TTR method and were presented here. The results were used to assess and discuss the influence of the deposition/growing method, and film thickness on the thermal characteristics of thin-films.

## REFERENCES

1. Burzo, M. G., P. L. Komarov, and P. E. Raad. 2002. "A Study of the Effect of Surface Metalization on Thermal Conductivity Measurements by the Transient Thermo-Reflectance Method," *ASME J. Heat Transfer*, 124(6):1009-1019.
2. Komarov, P. L., M. G. Burzo, G. Kaytaz, and P. E. Raad. 2003. "Transient Thermo-Reflectance Measurements of the Thermal Conductivity and Interface Resistance of Metallized Natural and Isotopically-Pure Silicon," *Microelectronics J.*, 34:1115-1118.
3. Tien, C. L., A. Majumdar, and F. M. Gerner (Eds.). 1998. *Microscale Energy Transport*, Taylor and Francis, Washington, DC.
4. Majumdar, A. 1993. "Microscale Heat Conduction in Dielectric Thin Films," *ASME J. Heat Transfer*, 115:7-16.
5. Capinski, W. S., and H. J. Maris. 1996. "Improved Apparatus for picosecond pump-and-probe optical measurements," *Review of Scientific Instruments*, 67(8):2720-2726.
6. Tzou, D. Y. 1997. *Macro- to Microscale Heat Transfer (The Lagging Behavior)*, Taylor and Francis, Washington, DC.
7. Hatta, I. 1990. "Thermal Diffusivity Measurements of Thin Films and Multilayered Composites," *International J. Thermophysics*, 11(2): 293-303.
8. Paddock, A., and G. L. Eesley. 1986. "Transient Thermorefectance from Thin Metal Films," *J. Applied Physics*, 60:285-290.
9. Capinski, W. S. and H. J. Maris. 1996. "Improved Apparatus for Picosecond Pump-and-probe Optical Measurements," *Review of Scientific Instruments*, 67:2720-2726.
10. Taketoshi, N., T. Baba, and A. Ono. 1999. "Observation of Heat Diffusion across Submicrometer Metal Thin Films Using a Picosecond Thermorefectance Technique," *Japanese J. of Applied Physics*, 38:L1268-L1271.
11. Qiu, T. Q., C. L. Tien. 1994. Femtosecond laser heating of multi-layer metals – I. Analysis, *International J. of Heat and Mass Transfer*, 37:2789-2798.
12. Hanus, J., J. Feinleb, and W.J. Scouler. 1967. "Low-energy Interband Transitions and Band Structures in Nickel," *Physical Review Letters*, 19(1):16-20.
13. Rosei, R., and D. W. Lynch. 1972. "Thermomodulation Spectra of Al, Au, and Cu," *Physics Review B*, 5:3883-3893.
14. Tessier, G., S. Hole, and D. Fournier. 2001. "Quantitative Thermal Imaging by Synchronous Thermorefectance with Optimized Illumination Wavelengths," *Applied Physics Letters*, 78:2267-2269.
15. Burzo, M. G., P. L. Komarov, and P. E. Raad. 2002. "Influence of a Metallic Absorption Layer on the Quality of Thermal Conductivity Measurements by the Transient Thermo-Reflectance Method," *Microelectronics Journal*, 33:697-703.
16. Powell, R. W., C. Y. Ho, and P. E. Liley. Nov. 1966. *Thermal Conductivity of Selected Solids*, NSRDS-NBS 8.
17. Burzo, M. G., P. L. Komarov, and P. E. Raad. 2002. "A Study of the Effect of Surface Metallization on Thermal Conductivity Measurements by the Transient Thermo-Reflectance Method," *ASME J. Heat Transfer*, 124:1009-1019.